JACS
JOURNAL OF THE AMERICAN CHEMICAL SOCIETY

Communication

pubs.acs.org/JACS

Photodissociation of B−N Lewis Adducts: A Partially Fused Trinaphthylborane with Dual Fluorescence

Kyohei Matsuo,[†] Shohei Saito,[†] and Shigehiro Yamaguchi*[,†,‡]

[†]Department of Chemistry, Graduate School of Science and [‡]Institute of Transformative Bio-Molecules (WPI-ITbM), Nagoya University, Furo, Chikusa, Nagoya 464-8602, Japan

Supporting Information

ABSTRACT: The synthesis of a planarized trinaphthylborane with partially fused structure is presented. This compound shows not only high chemical and thermal stability but also sufficient Lewis acidity to form Lewis adducts with pyridine derivatives in solution. The B−N Lewis adducts exhibit unprecedented photodissociation behavior in the excited state, reminiscent of the photogeneration of carbenium ions from triarylmethane leuco dyes. Consequently, these B−N Lewis adducts exhibit dual fluorescence emission arising from the initial tetracoordinate B−N adducts and the photodissociated tricoordinate boranes.

Incorporation of a tricoordinate, trivalent boron atom, which is isoelectronic to a carbenium ion, into π-conjugated skeletons enables the construction of charge-neutral electron-deficient molecules.[1] Boron-containing π systems readily react with Lewis bases to form the corresponding tetracoordinate species. This fundamental reactivity can be used to induce fascinating electronic properties and functions. In this context, a primary strategy is the generation of rigid π-conjugated skeletons with intense fluorescence by the intramolecular coordination with a *N*-heteroaryl group, such as in BODIPY and related dyes.[2] Recently, Wang et al. found an intriguing photorearrangement of intramolecularly *N*-heteroaryl-coordinated boron compounds, in which a boracyclopropane is formed, while the B−N bond remains intact.[3] Their intensive investigations on the scope of this reaction demonstrated a potential use for these compounds in new photochromic systems. In comparison, the reactivity of intermolecular complexes between boranes and neutral Lewis bases has not received much attention from a design perspective regarding functional materials. For this type of complex, Braunschweig, Engels, et al. recently reported an intriguing type of photoreactivity: a photomigration of an intermolecular complex between an electron-accepting borole and 2,6-lutidine.[4] Here, we would like to report yet another, unprecedented type of photoreactivity for intermolecularly coordinated triarylborane−pyridine complexes, which photodissociate in the excited state (Figure 1a) and exhibit dual fluorescence. While a laser photolysis of borane carbonyl (BH_3CO) is known as a similar type of reaction,[5] the present B−N photodissociation is reminiscent of the photogeneration of carbenium ions from triarylmethane leuco dyes.[6] Here, we disclose the synthesis of highly Lewis acidic trinaphthylborane **1** and the photodissociation of its Lewis base adducts with various pyridine derivatives.

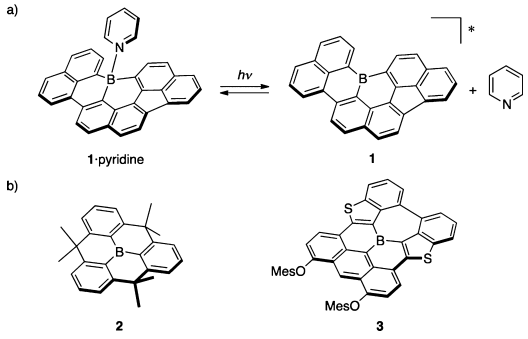

Figure 1. (a) Photodissociation of a partially fused trinaphthylborane **1**-pyridine complex and (b) the structures of some relevant planarized triarylboranes.

We recently demonstrated that the structural constraint arising from imposed planarity can be used as an efficient strategy for the stabilization of Lewis acidic triarylboranes, even in the absence of kinetic protection of the boron center (Figure 1b). Indeed, fully planarized triphenylborane **2** showed impressively high stability toward water, oxygen, silica gel, and amines.[7] We have also succeeded in the synthesis of some boron-embedded polycyclic π-conjugated compounds, such as **3** and a subunit of boron-doped graphene.[8] But in order to develop a more convenient synthetic pathway to structurally simpler boron-embedded π-skeletons, we attempted a 3-fold cyclization of tris(8-bromonaphthyl)borane **4** (Scheme 1). Thus, we treated a toluene solution of **4** with $(Me_3Si)_3SiH$ in the presence of 1,1′-azobis(cyclohexanecarbonitrile) (ABCN) as a radical initiator at 120 °C,[8a] which resulted in the formation of the partially fused trinaphthylborane **1** with an unexpected connectivity pattern with respect to the three naphthyl groups as the major product. Compound **1** was isolated as a red solid in 26% yield. Conversely, the expected fused product with C_3 symmetry was not observed, and no other byproducts were isolated. Although the detailed reaction mechanism still remains unclear, **1** is likely generated from successive intramolecular radical cyclizations,[9] followed by a skeletal rearrangement (Scheme S2).

Despite the partially fused framework, trinaphthylborane **1** showed notably high chemical stability. For example, even after more than one month in water-containing CH_2Cl_2, no

Received: July 10, 2014
Published: August 27, 2014

   dx.doi.org/10.1021/ja506980p | *J. Am. Chem. Soc.* 2014, 136, 12580−12583

Scheme 1. Synthesis and Derivatization of Trinaphthylborane 1

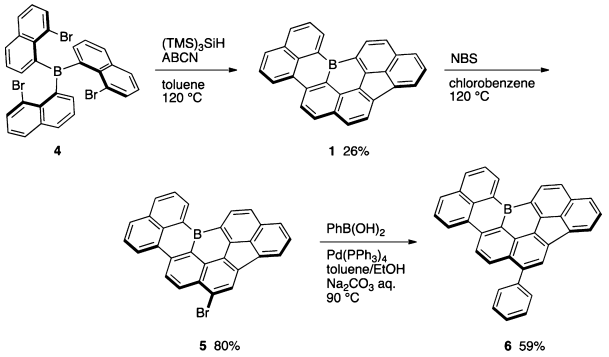

degradation was observed for **1**, as evident from UV−vis absorption measurements (Figure S10). This result is contrasted by the fact that the parent tri(1-naphthyl)borane rapidly ($t_{1/2}$ < 3 h) decomposes in CH_2Cl_2 solution in the air (Figure S11). But what is more important from a practical perspective is that the boron moiety in **1** remained intact during further functionalization reactions. For example, the electrophilic bromination of **1** with *N*-bromosuccinimide successfully afforded brominated **5** in 80% yield. A subsequent Suzuki−Miyaura cross-coupling between **5** and phenylboronic acid under basic aqueous conditions produced phenylated derivative **6** in 59% yield. The observed chemical tolerance is probably due to the chelating effect of the surrounding polycyclic framework and suggests the possibility to straightforwardly obtain a variety of derivatives of this trinaphthylborane core skeleton via well-established synthetic techniques. Furthermore, the high thermal stability of **1** was demonstrated by thermogravimetric analysis, which resulted in the determination of the decomposition temperature for a 5% weight loss (T_{d5}) under an N_2 atmosphere at 384 °C. Accordingly, it was possible to vacuum sublimate **1** at 250 °C/10^{-5} Torr.

The bond connectivity in the fused trinaphthylborane skeleton was unequivocally confirmed by X-ray crystallographic analysis of **5** (Figure 2a). Unfortunately, single crystals of the parent **1**

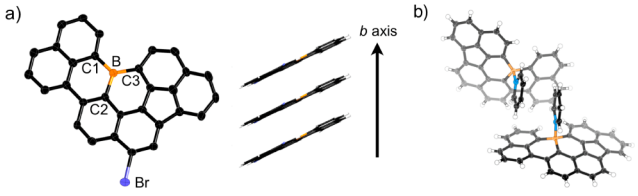

Figure 2. (a) Crystal structure (left) and the columnar packing (right) of **5**. A disordered Br atom is omitted for clarity (for the detail, see Supporting Information). (b) Crystal structure of **1**·pyridine. Thermal ellipsoids are drawn at the 50% probability.

could not be obtained. The crystallographic analysis of **5** confirmed that one of the three naphthyl groups is connected to the boron center in its 2-position. The three naphthyl groups are connected to each other via three $C(sp^2)-C(sp^2)$ bonds. Consequently, the compound forms a nine ring-fused $C_{30}B$ skeleton with a benzofluoranthene substructure. The central boron atom adopts a trigonal planar geometry. Overall, the fused trinaphthylborane skeleton adopts an almost planar geometry. The crystal packing of **5** is best described by a columnar π-stacked structure, where the average distance between planes is 3.45 Å. For air-stable triarylboranes, this is an unprecedented structural feature, and the ability to form columnar stacks would be beneficial for the construction of supramolecules or discotic liquid crystals. We evaluated carrier transporting properties as one of the fundamental properties of the stacked structure. A top-contact OFET device was fabricated by vacuum vapor deposition of **1**, which showed ambipolar carrier transporting abilities with a hole mobility of $\mu_h = 9.3 \times 10^{-6}$ cm^2 V^{-1} s^{-1} and an electron mobility of $\mu_e = 1.7 \times 10^{-5}$ cm^2 V^{-1} s^{-1} (Figures S6 and S7). Although the performance is poor, this is the first OFET of an air-stable triarylborane.

Another notable structural feature of **5** is the B−C bond lengths, which amount to 1.549(10), 1.567(10), and 1.603(10) Å. These bonds are longer than those in structurally constrained triphenylborane **2** (1.51−1.54 Å)[7a] and comparable to typical B−C bonds in unconstrained triarylboranes (1.57−1.59 Å).[10] This feature should be relevant to its Lewis acidity.

Upon addition of an excess of pyridine, the broad ^{11}B NMR signal of **1** at δ 46.8 ppm in chlorobenzene-d_5 completely disappeared in favor of an emerging sharp signal at δ −3.2 ppm, which was assigned to the **1**·pyridine adduct. The single crystals of the adduct suitable for X-ray diffraction analysis were obtained from vapor diffusion of heptane into a toluene/pyridine solution of **1** (Figure 2b). The asymmetric unit of these crystals contains two crystallographically independent molecules, both of which adopt a shallow bowl-shaped structure. The sum of the three C−B−C bond angles is 340.5° and 342.2°. The most notable feature in these molecules is the long B−N distance of 1.6927(17) and 1.6939(16) Å. These values are significantly higher than those in a sterically hindered dibenzoborole·pyridine adduct [1.638(4) Å],[11] a pentaphenylborole·2,6-lutidine adduct [1.6567(3) Å],[4] and a frustrated Lewis pair between $B(C_6F_5)_3$ and 2,6-lutidine [1.661(2) Å],[12] all of which dissociate in solution at room temperature. This comparison suggests a rather weak B−N coordination in **1**.

Despite the weak B−N coordination, the Lewis acidity of **1** is still higher than those of the previously reported structurally constrained triarylboranes. This fact was demonstrated by a titration experiment of **1** with pyridine monitored by UV−vis absorption spectroscopy (Figure 3a). A toluene solution of **1**

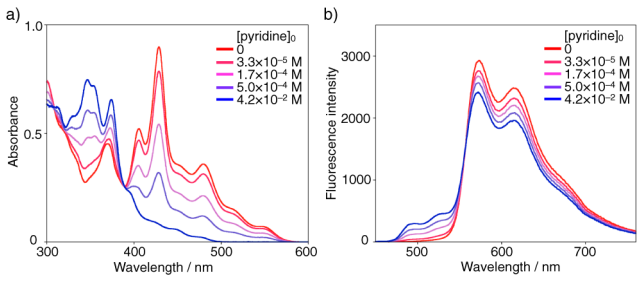

Figure 3. Titration of **1** in toluene ($[\mathbf{1}]_0 = 3.4 \times 10^{-5}$ M) with pyridine, measured by (a) UV−vis absorption and (b) fluorescence (λ_{ex} = 390 nm) spectroscopy.

showed its longest absorption maximum at 546 nm and another intense absorption at 429 nm. Upon addition of pyridine, these absorption bands gradually decreased, and new bands were observed at 346 and 374 nm, with a broad tail up to 490 nm. Isosbestic points were found at 390 and 309 nm. The significant hypsochromic shifts of the absorption maxima are due to the disruption of the π-conjugation through the p orbital at boron by the coordination of pyridine. Notably, the absorption bands of **1**

dx.doi.org/10.1021/ja506980p | J. Am. Chem. Soc. 2014, 136, 12580−12583

($[\mathbf{1}]_0 = 3.4 \times 10^{-5}$ M) beyond 500 nm completely disappeared after the addition of pyridine up to $[\text{pyridine}]_0 = 4.2 \times 10^{-2}$ M. This is, in contrast to the fully constrained **2** and **3**,[7a,8a] indicative of a quantitative formation of the **1**·pyridine adduct under the applied conditions. The binding constant of **1** toward pyridine (toluene/25 °C) was established to be 5.1×10^3 M^{-1} (Figure S12), which is much higher than that of **3** (0.35 M^{-1}, THF).[8a] The higher Lewis acidity of **1** relative to **3** should be attributed to the structural difference arising from the smaller constraint in **1**, rather than to the difference in electron-accepting properties. Cyclic voltammetry measurements in THF showed a lower first reduction potential for **1** (−1.48 V vs Fc/Fc^+; Figure S18) compared to **3** (−1.37 V).[8a]

The titration experiments of toluene solutions of **1** with pyridine were also monitored by fluorescence spectroscopy, which allowed us to observe an unexpected phenomenon (Figure 3b). In the absence of pyridine, the solution of **1** showed an orange emission band at 573 nm with a quantum yield of 0.15 and a lifetime of 10.7 ns. Upon the addition of pyridine, a new band for **1**·pyridine appeared at 500 nm, while the original emission band gradually decreased. This is consistent with the corresponding spectral change in the UV−vis absorption. However, the longer-wavelength emission band essentially remained present, and only slightly decreased in intensity, even after an excess of pyridine was added, which resulted in a complete disappearance of the absorption band associated with **1**. The excitation spectra monitored for the shorter and longer-wavelength emission bands were identical to each other as well as to the absorption spectrum of **1**·pyridine. Consequently, both the fluorescence bands should arise from the photoexcitation of **1**·pyridine. In other words, the Lewis adduct **1**·pyridine exhibits dual fluorescence.

Therefore, time-resolved fluorescence spectra of a toluene solution of **1**·pyridine were recorded at λ_{ex} = 377 nm (Figure S15). Immediately after the excitation, the first emission band appeared around 500 nm, and subsequently the longer-wavelength emission started to emerge. The fluorescence lifetime values for the two emission bands in the region of 470−510 and 560−660 nm were determined to be 2.3 and 11.0 ns, respectively, the latter of which is comparable to that of uncoordinated **1**. These results can be rationalized by considering the photodissociation of **1**·pyridine in the lowest singlet excited state (S_1; Figure 4). While the shorter-wavelength fluorescence arises from the locally excited state of **1**·pyridine, the photodissociation occurring in S_1 generates uncoordinated borane **1**, which is responsible for the longer-wavelength fluorescence emission. In the ground state, **1** immediately reforms the Lewis adduct, due to the presence of an excess of pyridine. Similar fluorescence properties have been reported for 9-phenylxanthen-9-ol, which undergoes photodehydroxylation under concomitant emission of dual fluorescence from the excited alcohol and the photodissociated carbenium ion.[13] Thus, it is the isoelectronic relationship between the carbenium ion and the tricoordinate borane, which determines the similar behavior in the excited state.

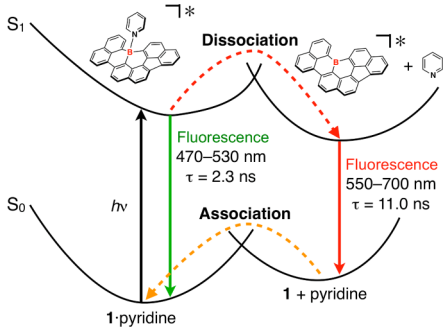

Figure 4. A plausible energy diagram for the photodissociation of **1**·pyridine.

To gain a deeper understanding of the excited-state behavior of **1**·pyridine, temperature- and solvent-dependent fluorescence spectra were recorded under the conditions that uncoordinated **1** was not observed in the absorption spectra. As the temperature decreased from 292 to 193 K, the shorter-wavelength emission band increased, while the one at longer wavelength decreased. The photodissociation is hence suppressed at low temperature, indicative of the presence of an activation barrier in S_1 for the photodissociation process (Figure S16). On the other hand, with increasing solvent polarity, the relative intensity of the shorter-wavelength emission band increased, whereas the absorption spectra showed only a subtle solvent dependence (Figure S17). These results demonstrate that the solvent polarity significantly affects the excited state and that the photodissociation becomes more unfavorable in polar solvents. According to TD-DFT calculations at the B3LYP/6-31G(d) level, the dipole moment of the optimized structure of **1**·pyridine in S_1 (7.8 D) is bigger than that of **1** in S_1 (1.5 D; Figures S28 and S30). Therefore, the nondissociated Lewis adduct is stabilized to a greater extent in polar solvents in S_1, relative to the dissociated borane species, resulting in a suppression of the dissociation.

We moreover conducted titration experiments of toluene solutions of **1** with various other Lewis bases (Figure 5). Initially,

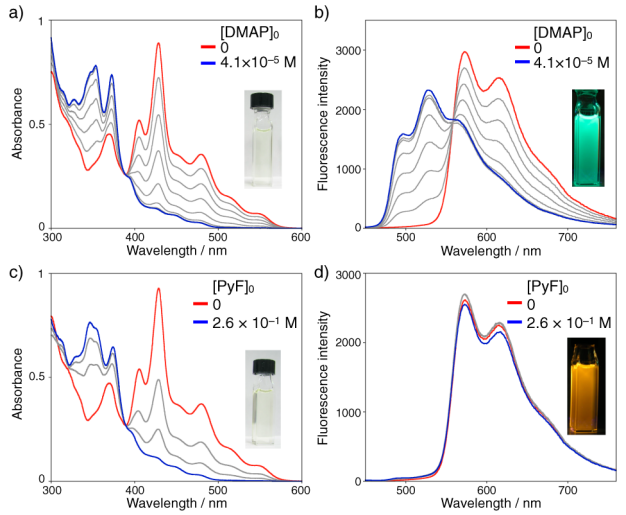

Figure 5. Titrations of toluene solutions of **1** ($[\mathbf{1}]_0 = 3 \times 10^{-5}$ M) with DMAP (a,b) and PyF (c,d) monitored by UV−vis absorption (a,c) and fluorescence spectroscopies (λ_{ex} = 390 nm) (b,d).

we substituted pyridine with the more Lewis basic *N,N*-dimethyl-4-aminopyridine (DMAP). Based on UV−vis spectroscopic titrations, the binding constant for **1** toward DMAP was estimated to be 6.6 (±1.3) × 10^6 M^{-1} (Figure S13). More importantly, we were unable to observe any photodissociation in the fluorescence spectra. Upon addition of DMAP to a toluene solution of **1**, both the absorption and fluorescence spectra were found to change proportionally to the amount of DMAP added. Ultimately, only one green emission band was observed at 527

dx.doi.org/10.1021/ja506980p | J. Am. Chem. Soc. 2014, 136, 12580−12583

nm, which was attributed to **1**·DMAP. In contrast, the use of the weaker Lewis basic 3-fluoropyridine (PyF) resulted in an almost unchanged fluorescence spectrum of **1**, even when an excess of PyF was added after the absorption band of **1** had completely changed into a new band of the **1**·PyF adduct. The binding constant of **1** toward PyF was determined to be 1.6×10^2 M^{-1} (Figure S14). These results demonstrate that the photodissociation behavior of these systems strongly depends on the Lewis basicity of the additive. The observed dual emission of **1**·pyridine is based on the delicate balance between the Lewis acidity of **1** and the Lewis basicity of the pyridine derivatives.

A highly relevant question in this context is how the Lewis basicity of the additive affects the behavior in the excited state. In order to shed some light on this question, DFT calculations at the B3LYP/6-31G(d) level were carried out for **1**·pyridine, **1**·DMAP, and **1**·PyF. The HOMOs of these compounds are comparable and are mainly localized on the benzofluoranthene moiety. The LUMOs of these compounds, on the other hand, are distinctly different. While the LUMO of **1**·DMAP is delocalized over the three naphthalene moieties, both **1**·pyridine and **1**·PyF exhibit LUMOs localized on the pyridine moieties (Figure S27). As a result, significantly different S_1 characters are observed. Based on TD-DFT calculations at the same level of theory, the S_1 of **1**·DMAP has a $\pi-\pi^*$ transition character, and therefore the photoexcitation does not affect the bonding nature of the pyridine−boron moiety. In contrast, **1**·pyridine and **1**·PyF exhibit an intramolecular charge transfer character from the benzofluoranthene moiety into the pyridine moiety in S_1. This difference should be responsible for the characteristic behavior in the excited state. However, the optimized structure of **1**·pyridine in S_1 obtained from the TD-DFT calculation at the B3LYP/6-31G(d) level suggests a much shorter B−N bond (1.592 Å) compared to the ground state (1.737 Å; Figures S23 and S31). This structural feature is apparently inconsistent with the photodissociation reactivity. How the borane−pyridine Lewis adducts actually undergo the photoinduced dissociation still remains to be determined.

In summary, we have synthesized a partially fused triarylborane **1**. The small structural constraint imparts high Lewis acidity to the planarized triarylborane skeleton, while the remarkable stability toward water and oxygen is maintained. Consequently, the molecule can easily form Lewis adducts in solution, even with weakly Lewis basic pyridine derivatives. Importantly, these B−N Lewis adducts undergo unprecedented photodissociation in the excited state, resulting in a dual emission that covers a broad range of the visible light (480−700 nm). The photoinduced B−N bond cleavage and the regeneration of the highly stable boron-embedded π systems should have great potential as a basis for various functions, such as photochromism, organocatalysis, and photoresponsive supramolecular assembly.[14] Further studies exploring these possibilities are currently undertaken in our laboratory.

■ ASSOCIATED CONTENT

Supporting Information

Experimental procedures and characterization data. This material is available free of charge via the Internet at http://pubs.acs.org.

■ AUTHOR INFORMATION

Corresponding Author

yamaguchi@chem.nagoya-u.ac.jp

Notes

The authors declare no competing financial interest.

■ ACKNOWLEDGMENTS

This work was partly supported by CREST, JST, and a Grant-in-Aid for Scientific Research on Innovative Area (Stimuli-responsive Chemical Species, no. 24109007) from the Ministry of Education, Culture, Sports, Science, and Technology (MEXT) of Japan. K.M. thanks the JSPS for a Research Fellowship for Young Scientists.

■ REFERENCES

(1) For reviews, see: (a) Entwistle, C. D.; Marder, T. B. *Angew. Chem., Int. Ed.* **2002**, *41*, 2927. (b) Entwistle, C. D.; Marder, T. B. *Chem. Mater.* **2004**, *16*, 4574. (c) Yamaguchi, S.; Wakamiya, A. *Pure Appl. Chem.* **2006**, *78*, 1413. (d) Bosdet, M. J. D.; Piers, W. E. *Can. J. Chem.* **2008**, *86*, 8. (e) Jäkle, F. *Chem. Rev.* **2010**, *110*, 3985. (f) Hudson, Z. M.; Wang, S. *Dalton Trans.* **2011**, *40*, 7805.

(2) For reviews, see: (a) Loudet, A.; Burgess, K. *Chem. Rev.* **2007**, *107*, 4891. (b) Ulrich, G.; Ziessel, R.; Harriman, A. *Angew. Chem., Int. Ed.* **2008**, *47*, 1184. (c) Rao, Y.-L.; Wang, S. *Inorg. Chem.* **2011**, *50*, 12263. (d) Frath, D.; Massue, J.; Ulrich, G.; Ziessel, R. *Angew. Chem., Int. Ed.* **2014**, *53*, 2290.

(3) (a) Rao, Y.-L.; Amarne, H.; Zhao, S.-B.; McCormick, T. M.; Martić, S.; Sun, Y.; Wang, R.-Y.; Wang, S. *J. Am. Chem. Soc.* **2008**, *130*, 12898. (b) Baik, C.; Hudson, Z. M.; Amarne, H.; Wang, S. *J. Am. Chem. Soc.* **2009**, *131*, 14549. (c) Rao, Y.-L.; Amarne, H.; Wang, S. *Coord. Chem. Rev.* **2012**, *256*, 759. (d) Rao, Y.-L.; Chen, L. D.; Mosey, N. J.; Wang, S. *J. Am. Chem. Soc.* **2012**, *134*, 11026. (e) Nagura, K.; Saito, S.; Fröhlich, R.; Glorius, F.; Yamaguchi, S. *Angew. Chem., Int. Ed.* **2012**, *51*, 7762. (f) Kropp, M.; Bhamidapaty, K.; Schuster, G. B. *J. Am. Chem. Soc.* **1988**, *110*, 6252.

(4) Ansorg, K.; Braunschweig, H.; Chiu, C.-W.; Engels, D.; Gamon, D.; Hügel, M.; Kupfer, T.; Radacki, K. *Angew. Chem., Int. Ed.* **2011**, *50*, 2833.

(5) Weiner, B. R.; Pasternack, L.; Nelson, H. H.; Prather, K. A.; Rosenfeld, R. N. *J. Phys. Chem.* **1990**, *94*, 4138.

(6) For reviews, see: (a) Bertelson, R. C. Photochromism. In *Techniques of Chemistry*; Brown, G. H., Ed.; Wiley-Interscience: New York, 1971; Vol. 3. (b) Das, P. K. *Chem. Rev.* **1993**, *93*, 119. (c) Duxbury, D. F. *Chem. Rev.* **1993**, *93*, 381.

(7) (a) Zhou, Z.; Wakamiya, A.; Kushida, T.; Yamaguchi, S. *J. Am. Chem. Soc.* **2012**, *134*, 4529. (b) Kushida, T.; Camacho, C.; Shuto, A.; Irle, S.; Muramatsu, M.; Katayama, T.; Ito, S.; Nagasawa, Y.; Miyasaka, H.; Sakuda, E.; Kitamura, N.; Zhou, Z.; Wakamiya, A.; Yamaguchi, S. *Chem. Sci.* **2014**, *5*, 1296.

(8) (a) Saito, S.; Matsuo, K.; Yamaguchi, S. *J. Am. Chem. Soc.* **2012**, *134*, 9130. (b) Dou, C.; Saito, S.; Matsuo, K.; Hisaki, I.; Yamaguchi, S. *Angew. Chem., Int. Ed.* **2012**, *51*, 12206.

(9) (a) Bowman, W. R.; Heaney, H.; Jordan, B. M. *Tetrahedron* **1991**, *47*, 10119. (b) Harrowven, D. C.; Sutton, B. J.; Coulton, S. *Tetrahedron* **2002**, *58*, 3387. (c) Majumdar, K. C.; Basu, P. K.; Chattopadhyay, S. K. *Tetrahedron* **2007**, *63*, 793 and references therein.

(10) (a) Zettler, F.; Hausen, H. D.; Hess, H. *J. Organomet. Chem.* **1974**, *72*, 157. (b) Blount, J. F.; Finocchiaro, P.; Gust, D.; Mislow, K. *J. Am. Chem. Soc.* **1973**, *95*, 7019. (c) Olmstead, M. M.; Power, P. P. *J. Am. Chem. Soc.* **1986**, *108*, 4235.

(11) Wehmschulte, R. J.; Khan, M. A.; Twamley, B.; Schiemenz, B. *Organometallics* **2001**, *20*, 844.

(12) Geier, S. J.; Gille, A. L.; Gilbert, T. M.; Stephan, D. W. *Inorg. Chem.* **2009**, *48*, 10466.

(13) Wan, P.; Yates, K.; Boyd, M. K. *J. Org. Chem.* **1985**, *50*, 2881.

(14) (a) Irie, M. *J. Am. Chem. Soc.* **1983**, *105*, 2078. (b) Kimura, K.; Mizutani, R.; Yokoyama, M.; Arakawa, R.; Sakurai, Y. *J. Am. Chem. Soc.* **2000**, *122*, 5448. (c) Liu, H.; Xu, Y.; Li, F.; Yang, Y.; Wang, W.; Song, Y.; Liu, D. *Angew. Chem., Int. Ed.* **2007**, *46*, 2515. (d) Wang, B. C.; Chen, Q.; Xu, H.; Wang, Z.; Zhang, X. *Adv. Mater.* **2010**, *22*, 2553.